Dalton Transactions

Synthesis and Structural Studies of Copper(II) Complex With N2S2 based N-Substituted Pendant Phosphonic Acid Arms

Journal:	*Dalton Transactions*
Manuscript ID	DT-ART-12-2019-004869.R2
Article Type:	Paper
Date Submitted by the Author:	21-Feb-2020
Complete List of Authors:	Taschner, Ian; Indiana University Northwest, Chemistry Aubuchon, Ethan; Indiana University Northwest, Chemistry Schrage, Briana; University of Akron, Chemistry Ziegler, Christopher; University of Akron, Department of Chemistry van der Est, Art; Brock University, Chemistry

ARTICLE

Synthesis and Structural Studies of Copper(II) Complex with N_2S_2 Based *N*-Substituted Pendant Phosphonic Acid Arms

Received 00th January 20xx,
Accepted 00th January 20xx

DOI: 10.1039/x0xx00000x

Ian S. Taschner*[a], Ethan Aubuchon[a], Briana R. Schrage[b], Christopher J. Ziegler[b] and Art van der Est[c]

The synthesis of a heteromacrocyclic bifunctional chelator with phosphonic acid pendent arms is presented along copper(II) complexation. Ligand **N_2S_2-POH** featuring *N,N'-bis*-substituted phosphonate pendent arms was isolated in respectable yields, characterized, and chelated to copper(II). Implementation of both Moedritzer-Irani and Kabachnik-Fields conditions using aza-thia macrocycle 1,8-dithia-4,11-diazacyclotetradecane afforded 1,8-dithia-4,11-diazacyclotetradecane-4,11-diyl-*bis*-(methylene)-*bis*-(phosphonic acid) (**N_2S_2-POH**). Kinetic NMR studies provided four acid dissociation constants with respect to hydronium ion concentration. Benesi-Hildebrand binding experiment provided a conditional formation constant of 2.8 x 10^4 M^{-1}. Heteromacrocycle **N_2S_2-POH** readily formed an encapsulated copper(II) chelate at room temperature, which was examined through EPR analysis.

Introduction

The use of radioisotopic chelates for positron emission tomography (PET) has been vital for observation of metabolic processes *in vivo*, facilitating confidence in diagnostic evaluation by health professionals.[1] Several metal radioisotopes are used, for example, ^{64}Cu intrinsically provides a unique decay profile ($t_{1/2}$ = 12.7 h, β^+: 19%, β^-: 38%) and can be readily complexed with an organic ligand to improve biodistribution. The desired properties of a radiometal chelate *in vivo* are both thermodynamically stability and passive kinetics.[2] The "ideal" metal-chelate for imaging should have immediate absorption, high tissue specificity, biological inertness, and complete-intact excretion.[3] Cyclam derivatives were one of the first successful chelates incorporated due to the high selectivity for copper, but have been shown to deposit the radioisotope, possibly through reduction of Cu(II) to Cu(I). Subsequent loss of Cu(I) from the ligand either through reductive activation of oxygen or loss via transmetalation will cause random radiometal deposition within tissues complicating the PET scan and diagnosis.[4]

Common macrocyclic chelating agents for complexation of ^{64}Cu include DOTA, NOTA, p-NH_2-Bn-NOTA, p-NH_2-Bn-DOTA, and cryptand SarAr (Figure 1).[5] Many research groups are expanding and tuning ligands to overcome the complications such as slow metal complexation, which is a setback when incorporating a bioconjugate peptide. Studies comparing peptide or antibody conjugates with different chelators have indicated that choice of ligand is critical, influencing radiolabeling, targeting, and pharmacokinetics.[6] The CB-TE2A-^{64}Cu chelate, reported by Weisman *et al.*, possessed high kinetic inertness and tissue selectivity but required the need for harsh conditions to enable chelation of ^{64}Cu(II) to CB-TE2A, limiting the ligands efficiency.[7] To mitigate the elevated temperature and slow chelation rate of CB-TE2A with ^{64}Cu, CB-TE2P (Figure 1) was used as an alternative bifunctional chelate, providing high kinetic inertness and thermodynamic stability under room temperature chelation conditions.[7]

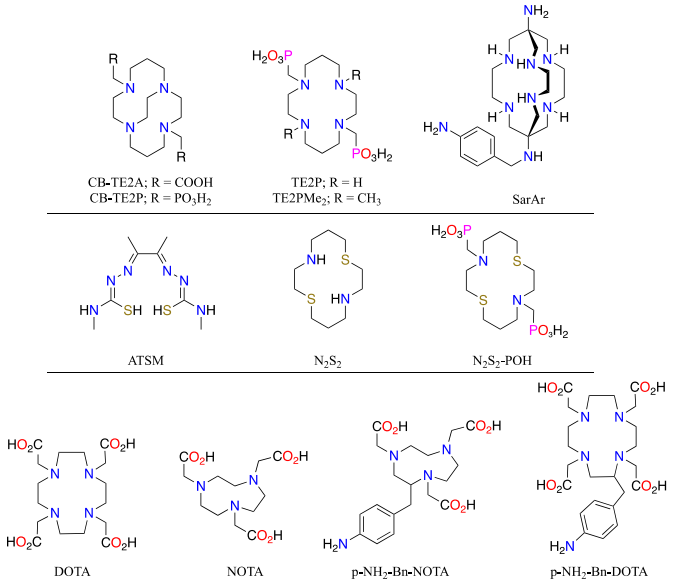

Figure 1 Heteromacrocyclic bifunctional chelators mentioned in the text

Chelation of copper(II) by a sarcophogine cage motif, SarAR, represents another class of ^{64}Cu ligands. Complexation of ^{64}Cu

[a] *Department of Chemistry, Indiana University Northwest, Gary, Indiana 46408, USA. E-mail: itaschne@iu.edu*
[b] *Department of Chemistry, The University of Akron, Akron, Ohio 44325, USA*
[c] *Department of Chemistry, Brock University, St. Catharines, ON L2S 3A1, Canada*
†Electronic Supplementary Information (ESI) available. See DOI: 10.1039/x0xx00000x

was complete within a few minutes over a wide range of pH values. The radiolabeled chelate, ^{64}Cu-SarAr, was reported to be completely cleared from the blood and liver over a 30 min period.[5] The radiopharmaceutical, ^{64}Cu-ATSM, incorporates two sulphur atoms in an acyclic chelate and has gained interest for imaging head[8], neck[8], lung[9], and cervical cancer[10]. ^{64}Cu-ATSM used in oncologic settings has been applied in detection of hypoxia as well as being a less invasive operation.[11] With a semithiocarbazone backbone, ^{64}Cu-ATSM, has high cell permeability and will diffuse into surrounding cells which undergoes a reduction in hypoxic cells selectively.[12]

With access to the **N_2S_2** backbone,[13] aspects of CB-TE2P, namely the 14-membered nitrogen containing macrocycle with pendant phosphonate arms could be combined with the sulphur heteroatoms from ATSM and investigated. Synthesis and physical properties of a new aza-thia macrocycle, **N_2S_2-POH**, was performed and reported herein.

Results and discussion

Synthesis

The synthesis of aza/thia-macrocycle **N_2S_2** was carried out on multi-gram scale in accordance with a previously reported synthetic sequence described by Walker *et al.*[14] The HCl salt of **N_2S_2-POH** was synthesized through two methods depicted in Scheme 1.

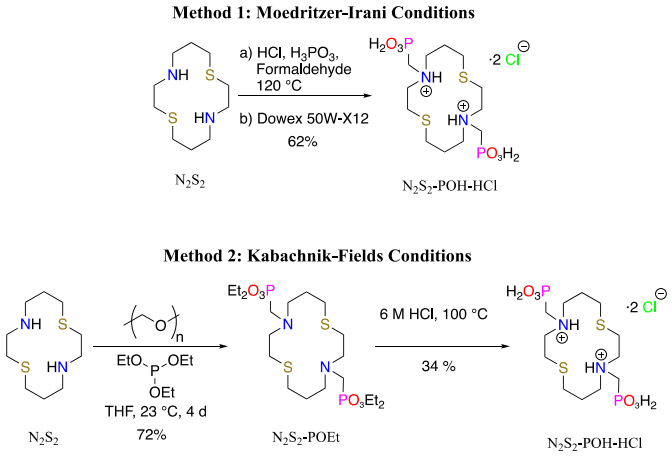

Scheme 1 Methods used for the synthesis of amino phosphonic acid **N_2S_2-POH-HCl**

Parent **N_2S_2** was subjected to Moedritzer-Irani conditions in a sealed tube to afford the target macrocyclic phosphonic acid **N_2S_2-POH-HCl**.[15] Crude NMR analysis revealed impurities and byproducts that could not be removed via crystallization. However, the use of a strong cation exchange resin (Dowex 50W-X12) with a 10% increase in acidic eluent per two column volumes provided **N_2S_2-POH-HCl** as a white solid. The second approach to the desired amino phosphonic acid was achieved through a Kabachnik-Fields reaction followed by acidic hydrolysis. The reaction of **N_2S_2** with paraformaldehyde and triethylphosphite, in THF provided **N_2S_2-POEt** in 72% yield after aqueous work up and column chromatography. Hydrolysis with 6 M HCl at 100 °C for 12 h afforded macrocyclic amino phosphonic acid **N_2S_2-POH-HCl** in 34% yield after ion exchange chromatography.

NMR Spectroscopy

The decomposition of **N_2S_2-POH-HCl** was observed during NMR analysis and initially attributed to impurities causing dephosphonylation. Both methods affording **N_2S_2-POH-HCl** subsequently underwent a slow retro-Moedritzer-Irani reaction in acidic media which limited the amount of time required to fully analyze the product spectroscopically. Dissolving **N_2S_2-POH-HCl** in 2 M aqueous carbonate, the **N_2S_2-POCs** and **N_2S_2-POK** salts (Scheme 2) were precipitated out through slow addition of an anti-solvent (methanol and ethanol respectively) at 0 °C. Macrocyclic salts **N_2S_2-POCs** and **N_2S_2-POK** were stable in aqueous media and provided high quality NMR spectra. Surprisingly, the formation of an ammonium salt in the presence of an excess of triethylamine, **N_2S_2-POH** produced the mono ammonium salt, **N_2S_2-PON** (Scheme 2), as determined through ^{1}H and ^{31}P NMR analysis. The formation of the mono ammonium adduct, **N_2S_2-PON**, prompted an investigation via dynamic NMR spectroscopy to determine the dissociation constants for the acidic protons. The potassium salt, **N_2S_2-POK,** at 25 mM was subjected to pH studies using 1 M $KOD_{(D2O)}$ to adjust the pH to 13 followed by 25 individual ~1 µL aliquots of 1 M $DCl_{(D2O)}$, providing four acid dissociation constants which agreed with literature values for similar macrocyclic aminophosphonic acids.[16]

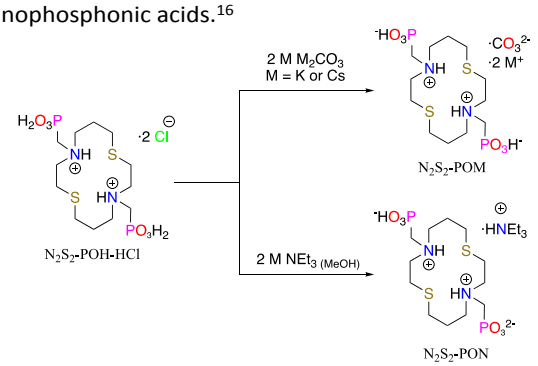

Scheme 2 Salt formation preventing retro-Moedritzer-Irani

The observed chemical shift is related to the frequencies of both acid (HA) and conjugate acid (A^-) through Equation 1. The frequency of a nucleus at equilibrium can be extrapolated to determine the mole fractions of HA and A^- at a set pH (Equation 3), where ν_{HA} and ν_{A^-} are the respective chemical shifts and x_{HA} and x_{A^-} are the respective mole fractions. The sum of the mole fractions must equal one (Equation 4), therefore determination of the acidic mole fraction (x_{HA}) can be used to estimate the desired acid dissociation constant. The acidic titrant utilized was 1 M DCl in D_2O and the pD was converted to pH using Equation 5. The dynamic pH spread of ^{1}H and ^{31}P NMR spectra are depicted in figure 2.

$$v_{obs} = v_{HA}(x_{HA}) + v_{A-}(x_{A-}) \quad (1)$$

$$pK_a = pH + log\frac{x_{HA}}{x_{A-}} \quad (2)$$

$$x_{A^-} = \frac{\nu(low\ pH) - \nu obs}{\nu(low\ pH) - \nu(high\ pH)} \quad (3)$$

$$x_{HA} + x_{A-} = 1 \quad (4)$$

$$pD = pH + 0.4 \quad (5)$$

Acid dissociation constants of **N_2S_2-POK** over a pH range of 0-13 were calculated using methodology outlined by Silva incorporating both ^{1}H and ^{31}P nuclear frequencies (Figure 2).[17] The acid dissociation constants were experimentally derived by varying solution pH and correlating chemical shift frequency (ν_{obs}). All ^{1}H frequencies of **N_2S_2-POK** were assigned, and four acid dissociation constants were obtained with suitable precision. Values for pK_{a1}-pK_{a4} associated with the ^{1}H's on the phosphonate moieties were 0.10 (±1.00), 4.47 (±0.05), 8.99 (±0.15), and 11.37 (±0.43), respectively. Chemical shift vs pH plots are presented in supplemental (Figure S2 and S3). Determination of the pKa values in solution of protioisomers **A**-**G** were accomplished by assuming that the major conformation in solution was *anti* with respect to the phosphonate pendant arms in relation to the aza-thia macrocyclic plane (Figure 3). Tentative conformers in solution at equilibrium with their respective protioisomer, **A**-**G**, could feasibly have the phosphonate pendant arms in a *syn*-orientation with respect to the aza-thia macrocycle, and stabilized through H-bonding or via metal coordination (pH dependent). The *syn* isomer **A'** is depicted in Figure 3, showing the possible equilibrium between *trans* conformer **A** in solution.

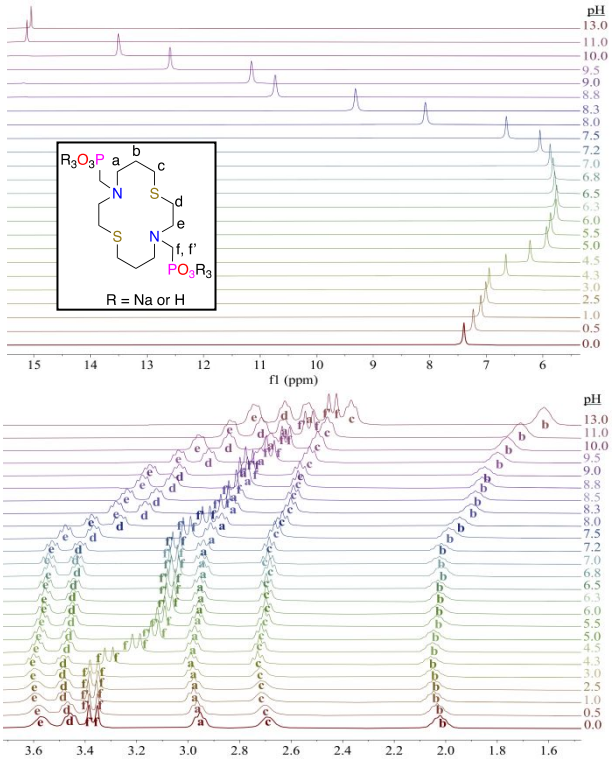

Figure 2 ^{31}P NMR at 25°C showing pH dependence on chemical shift (ν) of phosphorus nuclei (Top) and ^{1}H NMR at 25 °C showing dependence on chemical shift (ν).

Using the respective ^{1}H and ^{31}P frequencies, the mole fractions could be determined, thus providing an average pK_a for each protioisomer. Precise p$K_{a5\text{-}a6}$ values were difficult to obtain due to rotational impedance between -N-CH_2-P- at high ionic strength.[18]

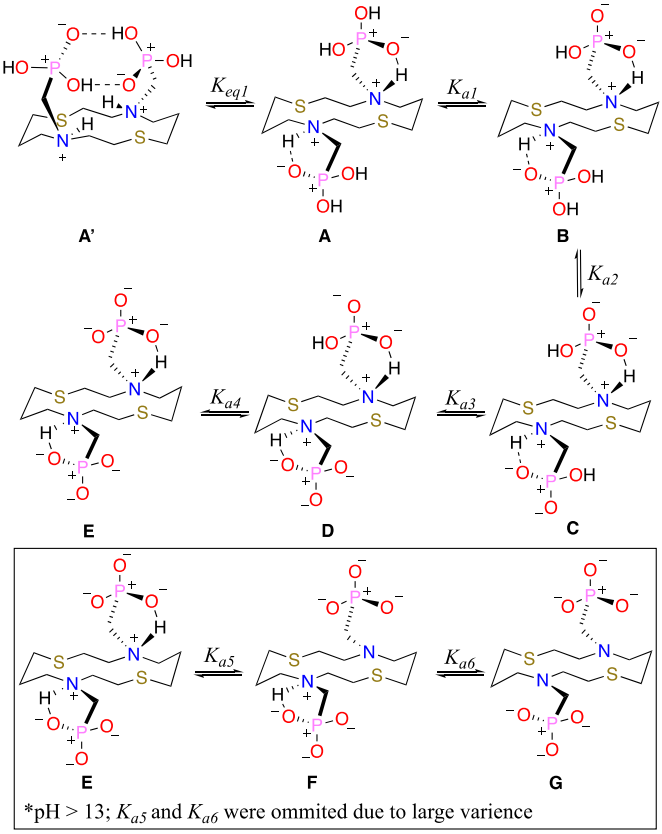

Figure 3 Proposed structural dynamics and associated Ka values and the depiction of *syn* isomer **A'**

The **N_2S_2-POK** ligand was exposed to a solution of copper(I) in acetonitrile-d_3, deuterium oxide, methanol-d_4 and chloroform-*d*, upon which all solutions immediately turned green and no signals were observed in the ^{1}H spectra. This possibly indicates that heteromacrocycle **N_2S_2-POK** has a strong preference for copper(II), and that at physiological pH copper(I) undergoes oxidation resulting in the copper(II) complex. Attempts to isolate the copper(I/II) salts for X-ray diffraction were unsuccessful.

Electrochemical Potential Measurements

The cyclic voltammograms of **N_2S_2-POK-Cu** and **N_2S_2-Cu** performed in 0.1 M NaOAc as the supporting electrolytic solution adjusted to pH = 7 are shown in Figure 4. The reduction of **N_2S_2-POK-Cu** is quasi-reversible with an $E_{1/2}$ value of -310 mV vs. Ag/AgCl corrected against the SHE (+0.197 V). The midpoint potential is ~-50 mV more negative than the corresponding **N_2S_2-Cu** complex. A comparison of the reported midpoint potential of **N_2S_2-Cu** in aqueous solution and a series of closely related complexes in acetonitrile indicate that this difference can be attributed largely to the stabilization of the Cu(I) species in acetonitrile.[19] Thus, the arrangement of the two sulfur and two nitrogen ligands does not appear to affect the midpoint potential strongly, and the potential can be attributed to the pendant arms of **N_2S_2-POK-Cu**.

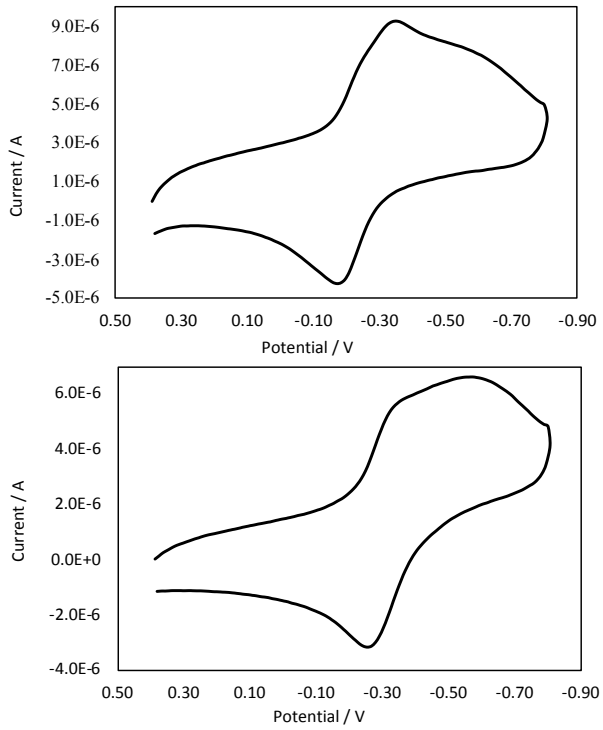

Figure 4 Cyclic voltammogram of N_2S_2.Cu (top) N_2S_2-POK-Cu (bottom) in H_2O. The data were collected with a 3 M Ag/AgCl (3 M NaCl) reference electrode, glossy carbon working electrode and platinum wire as auxiliary with a scan rate of 50 mV/s,. Background corrected using CV_EC Simulator v_17

EPR Measurements

The X-band EPR spectra of copper(II) acetate and **N_2S_2-POK-Cu** at 120 K in water:glycerol (80:20) are depicted in Figure 5. The copper acetate spectrum (A) shows a typical axial g-tensor pattern with four resolved hyperfine features on the low field end of the spectrum due to the large parallel component of the hyperfine coupling to *I*=3/2 Cu nucleus as expected for a square planar, or axially distorted octahedral geometry. The principal g-values and hyperfine couplings obtained from the spectrum ($g_{||}$=2.36, $g_{\perp}$=2.06, $A_{||}$ = 426 MHz, $A_{\perp}$ = 22 MHz) are in agreement with literature values[20] of copper acetate hexahydrate and are typical of copper(II) chelated with four oxygen atoms.[21]be g_{xx} = 2.01, g_{yy} = 2.07 and g_{zz} = 2.21 and the hyperfine coupling A_{zz} is ~330 MHz. A shift to lower *g*-value and the smaller hyperfine coupling is expected with a change from oxygen ligands to sulfur and nitrogen and the observed g_{zz} value is in line with that of axially symmetric Cu(II) centers with two nitrogen and two sulfur ligands.[21b] However, the rhombicity of the g-tensor and small value for A_{zz} indicate that a significant distortion of the structure from local D_{2h} symmetry must take place.

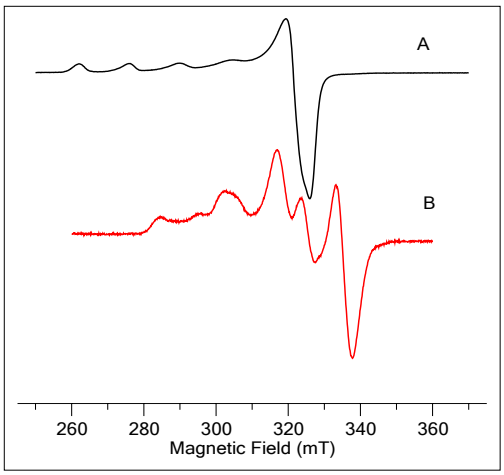

Figure 5 Continuous wave X-band EPR of A) $CuOAc_2$ and B) **N_2S_2-POK-Cu** at 120 K

Crystallography

Structural characteristics were further elucidated through single crystal X-ray diffractometry. An X-ray quality crystal was isolated through the use of an ethanol diffusion chamber. The crystal structures of **N_2S_2-POK** and **N_2S_2-HCl** are shown in Figure 6, each adopting a [3434] orientation according to Dale's nomenclature.[22] The structure of **N_2S_2-HCl** has been published previously.[13] The crystal system for **N_2S_2-POK** is monoclinic with the space group P-21/c. The hydrogen bonds are intermolecular between -N-H—O-P- each interacting with four other **N_2S_2-POK** ligands.

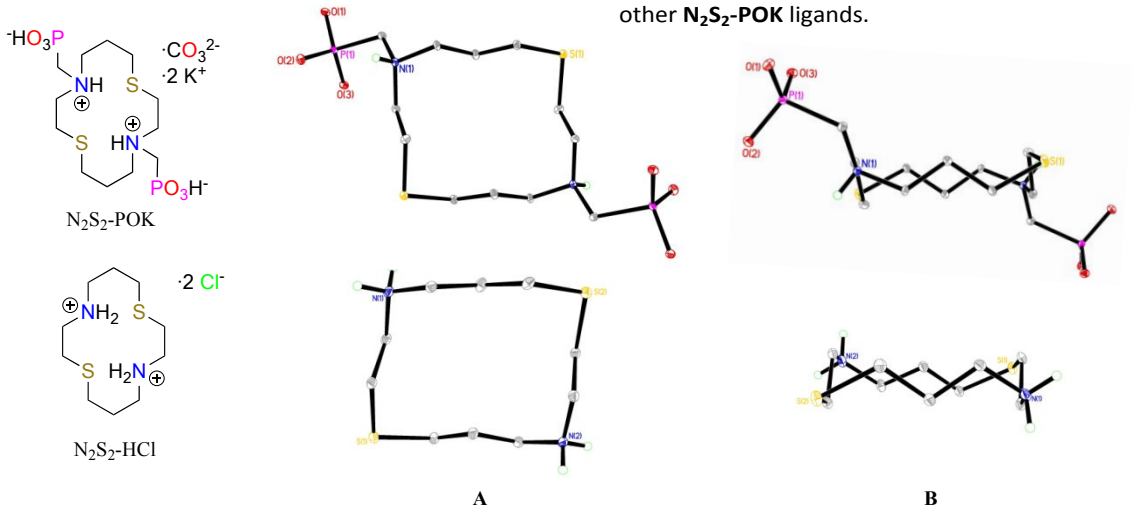

Figure 6 A) Thermal ellipsoid diagrams of N2S2-POK and previously reported N2S2-HCl (CCDC 888496) at 35% probability displacement ellipsoids showing [3434] conformation and B) macrocyclic crown conformation. All C-H hydrogen atoms are omitted for clarity.

A comparison of **N_2S_2** with **N_2S_2-POK** crystal data and structural refinement parameters are provided in supporting information along with key bond distances and angles (Table S1 and S2). The differences observed in topology between **N_2S_2-POK** and **N_2S_2-HCl** are heavily influenced by the associated amino-methylphosphonate pendant arm. The structural integrity of the "crown" conformation associated with **N_2S_2-HCl** is slightly compromised as well from the additional intermolecular H-bonds of the amino phosphonate moiety.

UV-Visible Spectra of Cu(II) Complex

The UV-visible spectrum of the copper adducts of **N_2S_2-POK** (Figure 7) exhibited λ_{max} of 246, 360, and 635 nm in aqueous media, comparable to previously reported data.[23] The absorption bands of copper bound **N_2S_2-POK** at 360 nm and 635 nm are slightly red shifted in comparison with **N_2S_2-Cu**. The absorption band at 360 nm corresponds to the S→Cu(II) ligand-to-metal charge transfer (LMCT), and the absorption at 635 nm results from the (N)→Cu(II) LMCT.[24] A blue shift was observed at 246 nm and can be attributed to the phosphonate pendant arms coordination with Cu(II).

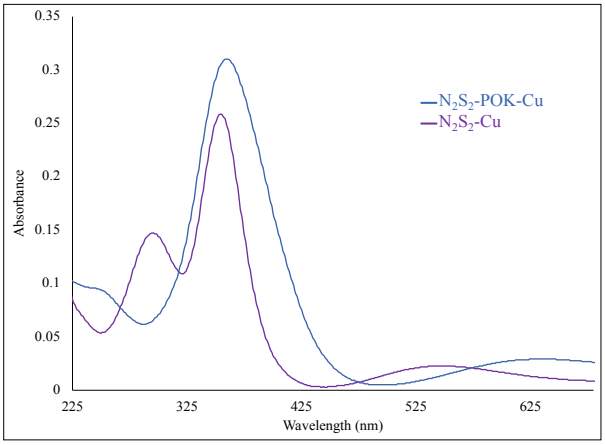

Figure 7 UV-Vis of N_2S_2-POK-Cu (purple) and N_2S_2-Cu (blue); pH 7, 0.1 M NaOAC

The conditional binding constant, K_{cond}^{HG}, was determined for **N_2S_2-POK-Cu** using a modified Benesi-Hildebrand[25] host:guest ([H]:[G]) study (Figure 8) through the following mathematical derivation:

$$H + G \rightleftharpoons HG$$

$$\Delta A = \frac{\Delta\varepsilon}{2}\left[\left([H]_O + [G]_O + \frac{1}{K}\right) \pm \sqrt{\left([H]_O + [G]_O + \frac{1}{K}\right)^2 - 4[H]_O[G]_O}\right] \quad (6)$$

Thermal binding constant, K_{therm}^{HG}, is determined from K_{cond}^{HG} through equation 7 using the equilibrium constants for binding of water to copper(II) and aqueous protonation constants associated with **N_2S_2-POK**, α_H, defined in the SI.

$$K_{therm}^{HG} = K_{cond}^{HG}\alpha_H \quad (7)$$

Where $[H]_0$ and $[G]_0$ are the analytical molar concentration of the host and guest, respectively. If $[G]_0$ is kept constant a plot of absorbance vs $[A]_0$ can be fit to equation 6 with the adjustable parameters of $\Delta\varepsilon$ and 1/K. Using equation 6 in tandem with a binding simulator[26] (Bindfit) the conditional association constant was determined to be 2.18 x 10^4 M^{-1} at 25 °C, at an ionic strength of 0.1 M H(K)Cl, and a $[H_3O]^+$ of 1 x 10^{-5}. This value was two orders of magnitude greater than previously reported parent **N_2S_2** (Table 1, NSNS) macrocycle.

Table 1. [14]ane macrocyclic stability constants and absorption bands for copper(II) complexes. Value in parenthesis was obtained using the procedure outlined in the SI.

Copper Ligate	pH	λ (nm)	K_{cond}, M^{-1}
S_4[23d, 27]	1	390	2.18 x 10^4
NSNS[27]	5	354	(6.7 x 10^2) 9.34 x 10^2
NSSN[23d]	2.3	335	1.07 x 10^4
NNNS[23d]	2.7	315	>1 x 10^5
NNSS[23d]	1.7	337	3.62 x 10^3
N_2S_2-POK	5	635	2.8 x 10^4

Complexation at 23 °C between **N_2S_2-POK** and copper perchlorate in an aqueous solution was complete within 3 minutes affording a dark green solution of **N_2S_2-POK-Cu**. This was performed at $[H_3O]^+$ concentrations between 10^{-3} – 10^{-7}. The increased complexation rate enables chelation to proceed under mild conditions allowing for potential peptide conjugates coupled to N_2S_2-POK for selective tissue delivery.

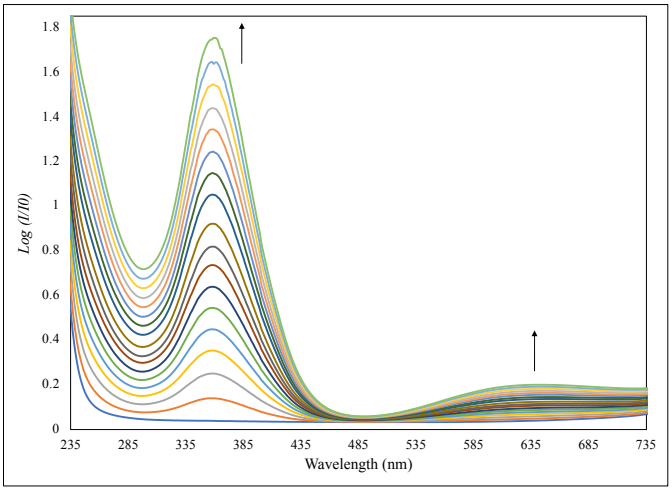

Figure 8 Benesi-Hildebrand Host:Guest UV-Vis spectra of **N_2S_2-POK-Cu** [0.03 M] $Cu(OCl_4)_2{\cdot}6\ H_2O$ [0.003 M].

Conclusions

Heteromacrocycle **N_2S_2-POK** was found to chelate and stabilize copper(II) in aqueous media within physiological pH and full complexation was complete within 3 min, which is comparable to macrocyclic amino phosphonates reported in literature.[27, Error! Bookmark not defined.] Comparison with parent **N_2S_2** macrocycle indicated slight perturbation of the rings structural topology and a more negative redox potential. The major difference was determined through a thermodynamic colorimetry experiment indicating the formation constant of **N_2S_2-POK** being two orders of magnitude greater than the **N_2S_2**. Cryptands based off of the **N_2S_2** macrocyclic scaffold will be prepared and evaluated against the SarAr copper ligate, which has high kinetic inertness and thermodynamic stability *in vivo*. Tuning of the **N_2S_2** macrocyclic backbone to obtain lower redox potentials, while

enhancing the thermodynamic and kinetic properties similar to the ^{64}Cu-ATSM ligand is of ongoing interest.

Experimental

All commercial reagents, unless otherwise stated, were used as received (Aldrich, VWR, or Fischer Scientific Ltd.). Dichloromethane and acetonitrile were distilled from calcium hydride under nitrogen. Dimethylformamide was distilled from calcium hydride under vacuum, stored over 3 Å molecular sieves, and degassed with argon using a gas dispersion frit. Reactions run at room temperature are in the range of 22–24 °C. ^{1}H and ^{13}C NMR spectra were obtained on a Varian 400 spectrometer as solutions in $CDCl_3$ and referenced to residual $CHCl_3$. For spectra taken in other NMR solvents, D_2O and DMSO-*d6*, the ^{1}H spectra were referenced to the residual solvent protioisomers, and ^{13}C spectra were referenced to the NMR solvent. Chemical shifts are expressed in parts per million values, and coupling constants (*J*) are reported in Hertz (Hz) and rounded to the nearest 0.5 Hz. The following abbreviations are used to indicate apparent multiplicities: s, singlet; d, doublet; dd, doublet of doublets; ddd, doublet of doublet of doublets; t, triplet; q, quartet; m, multiplet. Flash column chromatography on silica gel (60 Å, 230–400 mesh, low acidity, obtained from EMD Millipore Corporation) was performed using reagent grade solvents. Analytical thin-layer chromatography (TLC) was performed on precoated aluminum-backed silica gel plates (EMD Millipore Corporation), visualized with a UV lamp (254 nm) or iodine/silica or potassium molybdic acid solution in ethanol or $KMnO_{4(aq)}$ or *p*-anisaldehyde$_{(EtOH)}$ or vanillin$_{(EtOH)}$.

Physical Methods

FTIR spectra were collected on a Jasco 4600 spectrophotometer running Spectra Manager CFR®, where samples were prepared as a neat oil or solid on a ZnSe window using attenuated total reflectance (ATR). Melting points were obtained on a MeltTemp melting point apparatus and are uncorrected. High-resolution mass spectra (HRMS) were recorded on a time-of-flight JMS-T1000LC spectrometer with a DART ion source. ESI-MS spectra were acquired with a Bruker micrOTOF II, in the positive mode (parent ion plus H+). ESI samples were prepared for analysis by dissolving samples to 10^{-4} M in acetonitrile, and were directly infused into the mass spectrometer at a flow rate of 4 µL/min. The ESI was operated with a capillary offset of 4500 V, and a skimmer potential of 48 V. The samples were calibrated using an internal standard. X-ray intensity data were measured on a Bruker CCD-based diffractometer with dual Cu/Mo ImuS microfocus optics (Cu Kα radiation, λ = 1.54178 Å, Mo Kα radiation, λ =0.71073 Å). Crystals were mounted on a cryoloop using Paratone oil and placed under a steam of nitrogen at 100 K (Oxford Cryosystems). The data were corrected for absorption with the SADABS program. The structures were refined using the Bruker SHELXTL Software Package (Version 6.1), and were solved using direct methods until the final anisotropic full-matrix, least squares refinement of F2 converged. CCDC number 1969818 contains the supplementary crystallographic data for this paper. These data can be obtained free of charge from The Cambridge Crystallographic Data Centre via www.ccdc.cam.ac.uk/structures.

Electrochemistry

The cyclic voltammograms were collected using a BAS 100B Epsilon and C3 Cell Stand. Measurements were carried out in MilliQ water degassed for 20 min with nitrogen. A solution of 0.1 M sodium acetate in MilliQ water buffered to pH = 7 with glacial acetic acid was used as the supporting electrolyte. Cyclic voltammetry was recorded using a three-electrode system. A freshly polished glossy carbon was used as the working electrode with a 3 M NaCl Ag/AgCl reference electrode and a platinum auxiliary electrode. Voltammograms were cycled between −0.95 V to 0.95 V with scan rates of 50 mV/s.

EPR spectra were obtained using a modified ER 200D-SRC spectrometer with Bruker ER 041 X-MR microwave bridge and a dielectric resonator. The CW-EPR experiments were detected by 100 kHz field modulation and digitized by a Bruker 032 M signal channel. A 1 mM solution of the complex was prepared in 80% water and 20% glycerol solution and cooled to 120 K. Spectrometer microwave power was set to 1 mW and 10 G modulation amplitude.

Conflicts of Interest

There are no conflicts to declare

Acknowledgements

Ohio Board of Regents for funds used to purchase the Bruker-Nonius Apex CCD X-ray diffractometer and National Science Foundation (CHE-0840446). We thank the Indiana University Bloomington Mass Spectrometry Facility for exact mass measurements.

References

1 Rich, D. A brief history of positron emission tomography. *J. Nuc. Med. Tech.* **1997**, *25*, 4-11.

2 a) Dearling, J. L.; Voss, S.D.; Dunning, P.; Snay, E.; Fahey, F.; Smith, S. V.; Huston, J. S.; Meares, C. F.; Treves, T. S.; Packard, A. B. Imaging cancer using PET - the effect of the bifunctional chelator on the biodistribution of a ^{64}Cu-labeled antibody. *Nucl. Med. Biol*. **2011**, *38*(1), 29–38. b) Boswell, A. C.; Sun, X.; Niu, W.; Weisman, G. R.; Wong, E. H.; Rheingold, A. L.; Anderson, C. J. Comparative *in vivo* stability of coper-64-labeled cross-bridged and conventional tetraazamacrocyclic complexes. *J. Med. Chem.* **2004**, *47*(6), 1465-1474.

3 Sattelberger, A.P.; Atcher, R.W. Nuclear medicine finds the right chemistry. *Nat. Biotechnol*. **1999**, *17*, 849-850. b) Pomper, M. G. *Imaging in Oncology*; Gelovani, J. G., Ed.; CRC Press, New York, 2008, pp 300-304.

4 Wadas, T. J.; Wong, E. H.; Weisman, G. R.; Anderson, C. J. Copper chelation chemistry and its role in copper radiopharmaceuticals. *Curr. Pharm. Design.* **2007**, *13*, 3-16.

5 Anderson, C. J.; Ferdani, R. Copper-64 radiopharmaceuticals for PET imaging of cancer: Advances in preclinical and clinical research. *Cancer Biother. Radiopharm.*, **2009**, *24*, 379-393.

6 Bass, L. A.; Wang, M.; Welch, M. J.; Anderson, C. J. In vivo transchelation of copper-64 from TETA-octreotide to superoxide dismutase in rat liver. *Bioconjugate Chem*. **2000**, *11*, 527-532.

7 Stigers, D. J.; Ferdani, R.; Weisman, G. R.; Wong, E. H.; Anderson, C. J.; Golen, J. A.; Moore, C.; Rheingold, A. L. A new phosphonate pendant-armed cross-bridged tetraamine chelator accelerates copper(II) binding for radiopharmaceutical applications. *Dalton Trans.*, **2010**, *39*, 1699-1701.

8 Mccall, K. C.; Humm, J. L.; Bartlett, R.; Reese, M.; Carlin, S. Copper-64-diacetyl-bis (N(4)- methylthiosemicarbazone) pharmacokinetics in FaDu xenograft tumors and correlation with microscopic markers of hypoxia. *Int J Radiat Oncol Biol Phys.* **2012**, *84*(3), 393–399.

9 Lopci, E.; Grassi, I.; Rubello, D. Prognostic evaluation of disease outcome in solid tumors investigated with 64Cu-ATSM PET/CT. *Clin. Nucl. Med.* **2016**, *41*(2), 87–92.

10 Lewis, J. S.; Laforest, R.; Dehdashti, F.; Grigsby, P. W.; Welch, M. J.; Siegel, B. A. An imaging comparison of ^{64}Cu-ATSM and ^{60}Cu-ATSM in cancer of the uterine cervix. *J Nucl Med.* **2008**, *49*(7), 1177–1182.

11 Burgman, P.; O'Donoghuea, J. A.; Lewis, J. S.; Welch, M. J.; Humm, J. L.; Ling, C. C. Cell line-dependent differences in uptake and retention of the hypoxia-selective nuclear imaging agent Cu-ATSM. *Nuc. Med. Bio.* **2005**, *32*, 623-630.

12 Fujibayashi, Y.; Taniuchi, H.; Yonekura, Y.; Ohtani, H. Copper-62-ATSM: A new hypoxia imaging agent with high membrane permeability and low redox potential. *J. Nuc. Med.* **1997**, *38*, 1155-1160.

13 a) Taschner, I. S.; Walker, T. L.; DeHaan, H. S.; Schrage, B. R., Ziegler, C. J.; Taschner, M. J. Synthesis, Characterization, and Copper (II) Chelates of 1,11-Dithia-4,8-diazacyclotetradecane. *J. Org. Chem.* **2019**, *84*(17), 11091-11102. b) Walker, T. L.; Taschner, I. S.; Chandra, S. M.; Taschner, M. J.; Engle, J. T.; Schrage, B. R.; Ziegler, C. J.; Gao, X. Lone-Pair-Induced Topicity Observed in Macrobicyclic Tetra-thia Lactams and Cryptands: Synthesis, Spectral Identification, and Computational Assessment. *J. Org. Chem.* **2018**, *83*(17), 10025-10036.

14 Walker, T. L.; Malasi, W.; Bhide, S.; Parter, T.; Zhang, D.; Freedman, A.; Modarelli, J. M.; Engle, J. T.; Ziegler, C. J.; Custer, P.; Youngs, W. J.; Taschner, M. J. Synthesis and characterization of 1,8-dithia-4,11-diazacyclotetradecane. *Tetrahedron Lett*. **2012**, *53*, 6548-6551.

15 Turrin, C-O.; Hameau, A.; Caminade, A-M. Application of the Kabachnik–Fields and Moedritzer–Irani Procedures for the Preparation of Bis(phosphonomethyl)amino- and Bis[(dimethoxyphosphoryl)- methyl]amino-Terminated Poly(ethylene glycol). *Synthesis*. **2012**, *44*, 1628-1630.

16 Delgado, R.; Siegfried, L. C.; Kaden, T. A. 14. Metal Complexes with Macrocyclic Ligands: Protonation Studies and Complexation Properties of Tetraazamacrocyclic Methylenephosphonates with Earth-Alkali Ions. *Helvetica Chim. Acta.* **1990**, *73*, 140-148.

17 Delgado, R.; Fraústo da Silva, J.J.R.; Amorim, M.T.S.; Cabral, M.F.; Chaves, S.; Costa, J. Dissociation constants of Brønsted acids in D2O and H2O: Studies on polyaza and polyoxa-polyaza macrocycles and a general correlation. *Anal. Chim. Acta.* **1991**, *245*, 271–282.

18 Kotek, J.; Vojtisek, P.; Cisarova, I.; Hermann, P.; Jurecka, P.; Rohovec, J.; Lukes, I. Bis(methylphosphonic acid) derivatives of 1,4,8,11-tetraazacyclotetradecane (Cyclam). Synthesis, crystal and molecular structures, and solution properties. *Collect. Czech. Chem. Commun.* **2000**, *65*, 1289-1316.

19 a) Bernardo, M. M.; Heeg, M. J.; Schroeder, R. R.; Ochrymowycz, L. A.; Rorabacher, D. B. Comparison of the influence of saturated nitrogen and sulfur donor atoms on the properties of copper(II/I)-macrocyclic polyamino polythiaether ligand complexes: redox potentials and protonation and stability constants of CuIL species and new structural data. *Inorg. Chem.*, **1992**, *31*, 191–198. b) Pavlishchuk, V. V.; Yatsimirskii, K. B.; Strizhak, P. E. Redox behaviour of copper(II) tetrathia macrocyclic complexes. *Inorg. Chim. Acta* **1989**, *164*, 65–68.

20 Adams, R.; Gaura, R.; Raczkowski, R.; Kokoszka, G. EPR of a one-dimensional system: calcium copper acetate hexahydrate. *Phys. Lett. A*. **1974**, *49*(1), 11-12.

21 a) R. S. Drago, Physical Methods in Chemistry, Saunders, Philidelphia, PA, 2nd ed, **1977**, 13-2. b) Peisach, J.; Blumberg, W. E. Structural implications derived from the analysis of electron

paramagnetic resonance spectra of natural and artificial copper proteins. *Arch. Biochem. Biophys*. **1974**, *165*(2), 691-708.

22 Dale, J. Exploratory calculations of medium and large rings. Part 1. Conformational minima of cycloalkanes. *Acta Chem. Scand.* **1973**, *27*, 1115.

23 a) Waknine, D.; Heeg, M. J.; Endicott, J. F.; Ochrymowycz, L. A. Tetradentate macrocyclic complexes of platinum. X-ray crystal structure and redox behavior of complexes containing nitrogen or sulfur donor atoms. *Inorg. Chem.* **1991**, 3691-3700. b) Galijasevic, S.; Krylova, K.; Koenigbauer, M. J.; Jaeger, G. S.; Bushendorf, J. D.; Heeg, M. J.; Ochrymowycz, L. A.; Taschner, M. J.; Rorabacher, D. B. Chelate ring sequence effects on thermodynamic, kinetic and electron-transfer properties of copper (II/I) systems involving macrocyclic ligands with S4 and NS3 donor sets. *Dalton Trans.* **2003**, 1577-1586. c) Semira, G. Thermodynamic and electron-transfer properties of copper(II/I) polyaminothiaether complexes. *Transit. Met. Chem.* **2013**, *38*(8), 883-890. d) Westerby, B. C.; Juntunen, K. L.; Leggett, Gregory H.; Pett, V.B.; Koenigbauer, M. J.; Purgett, M. D.; Taschner, M. J.; Ochrymowycz, L. A.; Rorabacher, D. B. Macrocyclic polyamino polythiaether ligands with NxS4-x and NxS5-x donor sets: protonation constants, stability constants, and kinetics of complex formation with the aquocopper(II) ion. *Inorg. Chem.* **1991**, *30*(9), 2109-2120.

24 a) Rorabacher, D. B.; M. J. Martin, M.J.; Koenig Bauer, M.; Malik, R. R.; Schroeder, J. F.; Ochrymowycz, L .A. Copper Coordination Chemistry: Biochemical and Inorganic Perspectives, eds. K. D. Karlin and J. Zubieta, Academic Press, New York, **1983**, 167. b) Siegfried, L.; Kaden, T. A. Metal complexes with macrocyclic ligands. Part XIX. Synthesis and Cu2+ complexes of a series of 12-, 14-, and 16-membered cis-and trans-N2S2-macrocycles. *Helv. Chim. Acta.* **1984**, *67*, 29.

25 Benesi, H. A.; Hildebrand, J. H. "A Spectrophotometric Investigation of the Interaction of Iodine with Aromatic Hydrocarbons. *J. Am. Chem. Soc.* **1949**, *71* (8), 2703–2707.

26 a) Thordarson, P. Determining association constants from titration experiments in supramolecular chemistry. *Chem. Soc. Rev.* **2011**, *40*, 1305-1323. b) Hibbert, B. D.; Thordarson, P. The death of the Job Plot, transparency, open science and online tools, uncertainty estimation methods and other developments in supramolecular chemistry data analysis. *Chem. Commun.* **2016**, *52*, 12792-12805. c) Data fit, fit method, and optimization available at: http://app.supramolecular.org/bindfit/view/76602353-6efd-40e4-a457-09822d12d564

27 Walker, T. L.; Malasi, W.; Mula, S.; Van der Est, A.; Engle, J. T.; Ziegler, C. J.; Taschner, M. J. Blue copper protein analogue: synthesis and characterization of copper complexes of the N_2S_2 macrocycle 1,8-dithia-4,11-diazacyclotetradecane. *J. Chem. Soc., Dalton Trans.* **2015**, *44*, 20200-20206.

Physical properties and copper chelation of phosphonic acid substituted 14-[Ane]N_2S_2 macrocycle for use as a potential radio imaging ligand.

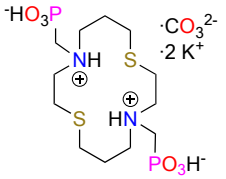

N_2S_2-POK

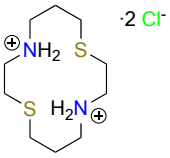

N_2S_2-HCl